

Energy-based seismic design of buckling-restrained braced frames using hysteretic energy spectrum

Hyunhoon Choi, Jinkoo Kim*

Department of Architectural Engineering, Sungkyunkwan University, Suwon, Republic of Korea

Received 12 November 2004; received in revised form 29 July 2005; accepted 11 August 2005

Available online 10 October 2005

Abstract

An energy-based seismic design procedure for framed structures with buckling-restrained braces is proposed using hysteretic energy spectra and accumulated ductility spectra. The procedure is based on the premise that the gravity load-resisting elements, such as beams and columns, are designed to remain elastic during earthquake, and all the seismic input energy is dissipated by the buckling-restrained braces. The proposed design procedure requires hysteretic energy spectra and accumulated ductility spectra corresponding to various target ductility ratios. The cross-sectional area of braces required to meet a given target displacement is obtained by equating the hysteretic energy demand to the accumulated plastic energy dissipated by braces. The design procedure was applied to three- and eight-story framed structures with buckling-restrained braces. Twenty earthquake records were utilized to construct the spectra and to verify the validity of the design procedure. According to analysis results, the mean values for the top story displacement correspond well with the given performance target displacements. Also, the inter-story drifts turned out to be relatively uniform over the structure height, which is desirable because uniform inter-story drifts indicate uniform damage distribution. © 2005 Elsevier Ltd. All rights reserved.

Keywords: Energy-based design; Hysteretic energy spectrum; Accumulated ductility; Buckling-restrained braces; Seismic design

1. Introduction

The current seismic design procedure allows inelastic deformation of structures to withstand the extra earthquake force in excess of the design force. This design concept, which is developed based on a monotonic loading condition, does not take into account the cumulative damage caused by earthquake ground excitation with hysteretic characteristics. As we have observed previously, this will lead to unexpected damage in structures for earthquake load even slightly larger than the design load. The performance-based seismic design method, such as a direct displacement-based design method, is considered to be a more advanced design methodology because it accounts for, although indirectly, the energy dissipation due to inelastic deformation. However, it has limitation in that only maximum responses are considered in the design process.

The energy-based seismic design methods, which utilize hysteretic energy of a structure as a main design parameter,

have been developed as potential alternatives to the conventional maximum value-based seismic design method. The method is rational in that the accumulation of earthquake-induced damage can be taken into account in the design procedure. Since the concept of energy was introduced by Housner [1] in seismic design, a lot of effort has been made in the field of energy-based seismic engineering. Uang and Bertero [2] and Estes and Anderson [3] obtained story-wise distribution of hysteretic energy in multi-story structures. Riddell and Garcia [4] presented a procedure for construction of a hysteretic energy demand spectrum. Léger and Dussault [5] investigated the influence of the mathematical modeling of viscous damping on the energy dissipation of structures. Akbas et al. [6] proposed a design procedure to dissipate input seismic energy by cumulative plastic rotation at the ends of beams. They assumed that the dissipated energy was distributed linearly along the building height. Leelataviwat et al. [7] proposed a seismic design method based on the energy balance concept. Most of the above mentioned research was limited to moment-resisting frames.

Recently Dasgupta et al. [8] applied the energy balance concept to compute the seismic design base shear of a

* Corresponding author.

E-mail address: jinkoo@skku.ac.kr (J. Kim).

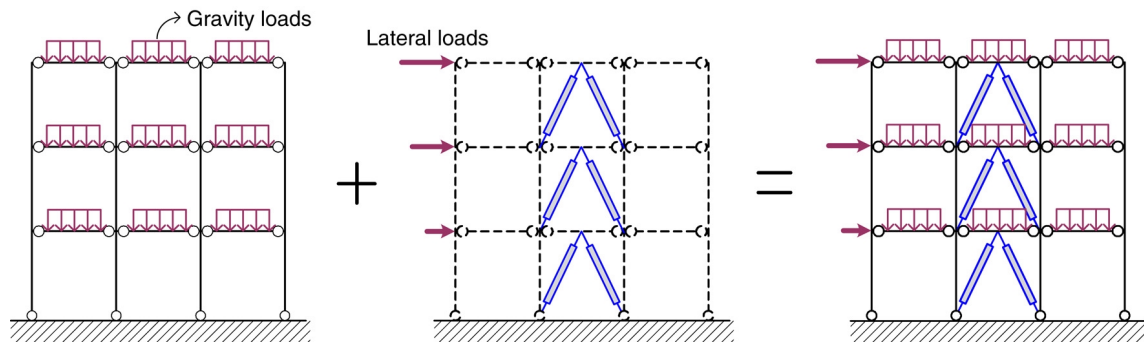


Fig. 1. Schematic of a framed structure with BRB.

buckling-restrained braced frame (BRBF), and found that the base shear obtained was significantly smaller than that obtained from the displacement-based design approach. Kim et al. [9] used the energy-balance concept to determine the size of buckling-restrained braces (BRB) in such a way that the hysteretic energy demand was equal to the energy dissipated by the BRB. However, the energy balance concept, although simple and convenient for energy based design, has the following fundamental limitations: In the equation proposed by Housner [1], the use of pseudovelocity for estimation of the input seismic energy sometimes significantly underestimates the input energy demand [2]. To enhance accuracy in the estimation of input energy, various methods were proposed by many researchers [10–12], which complicates the design procedure due to the involvement of many variables. Also as pointed out by Fajfar and Vidic [13] the input energy for a period range of practical structures tends to decrease as the ductility of the structure increases. However, the Housner's equation for computing seismic input energy cannot consider this phenomenon.

In this study seismic design procedure for framed structures with buckling-restrained braces (BRB) was proposed using hysteretic energy spectra and accumulated ductility spectra. It is assumed in the design process that the gravity load-resisting system, such as beams and columns, remains elastic during earthquake, and all the seismic input energy is dissipated by the BRB. The proposed design procedure is considered to be more accurate than the one based on the energy balance concept in that the hysteretic energy, which needs to be dissipated by the BRB, is not computed by the approximate formula proposed by Housner but obtained directly from the hysteretic energy spectrum constructed by a series of time-history analyses. To this end the hysteretic energy spectra corresponding to various target ductility ratios were constructed first. Accumulated ductility spectra, in which ductility ratios accumulated during an earthquake excitation are presented, were also plotted for various target ductilities. The cross-sectional area of BRB required to meet a given target displacement was obtained by equating the hysteretic energy demand to the plastic energy dissipated by braces. Twenty earthquake records were utilized to construct the spectra and to verify the validity of the design procedure.

2. Structure with buckling-restrained braces

BRB usually consist of a steel core undergoing significant inelastic deformation when subjected to strong earthquake

loads and a casing for restraining global and local buckling of the core element. According to previous research [14,15], a BRB exhibits stable hysteretic behavior with superior energy dissipation capacity. Most of the research, however, has been focused on experiments to investigate the energy dissipation capacity of the BRB elements, and further research is still required for development of a system level design procedure to apply BRB as an economic means of seismic design.

Fig. 1 shows the schematic of a structure with BRB, in which the beams and columns are designed to remain elastic under the earthquake load and the BRB are designed to dissipate all the input energy. As energy dissipation and the resultant damage are concentrated on braces, the demand for inelastic deformation and the damage in the main structural members are reduced significantly. The structure system has an advantage in that the braces can easily be replaced with new ones after damage by major earthquakes.

3. Hysteretic energy spectrum and accumulated ductility spectrum

In this section the procedure for constructing a constant ductility hysteretic energy spectrum and an accumulated ductility spectrum is addressed. An inelastic single-degree-of-freedom (SDOF) system with a given natural period and ductility ratio is selected. The elastic stiffness of the structure is obtained from the natural period and mass, and the elastic strength of the system is computed from time-history analysis assuming that the structure behaves elastically under earthquake excitation. Then for the inelastic system with a certain ratio of the yield strength and the elastic strength, the maximum displacement and the corresponding ductility ratio are computed. If the maximum ductility ratio is not close to the given target ductility ratio, the system is analyzed again with a different strength ratio. The process is repeated until the maximum and the target ductility ratios become nearly identical. After this process is completed the hysteretic energy of the inelastic system is finally computed.

The hysteretic energy dissipated in a structure depends on the amount of plastic deformation. Therefore to design a structure using a hysteretic energy spectrum, the amount of accumulated plastic deformation needs to be known. Such information can easily be acquired from an accumulated ductility spectrum, in which ductility ratios accumulated during

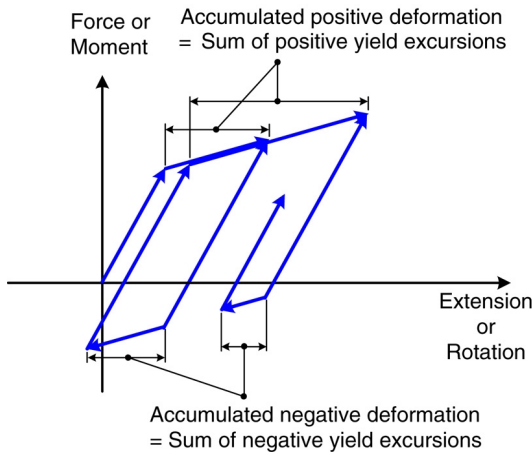


Fig. 2. Accumulated plastic deformation.

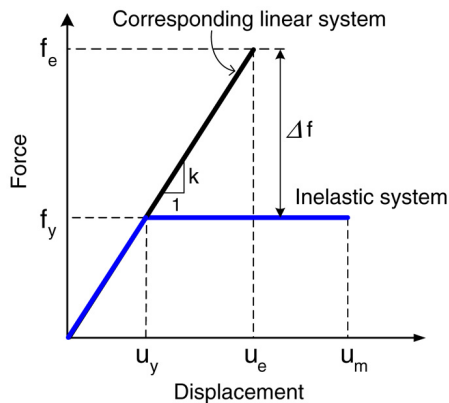


Fig. 3. Force–displacement relationship of an elasto-plastic system and the corresponding linear system.

an earthquake excitation are plotted for SDOF structures with various natural periods and target ductility ratios. The accumulated ductility is obtained by summation of positive and negative yield excursions shown in Fig. 2. Fig. 3 shows the force–displacement relationship of an elasto-plastic system, and Fig. 4 presents the flow-chart of constructing hysteretic energy and accumulated ductility spectra for elasto-plastic systems corresponding to specified ductility ratios.

Twenty ground motions developed for use in the FEMA/SAC project on steel moment-resisting frames located on soft rock sites [16] were utilized for construction of hysteretic energy and accumulated ductility spectra. Fig. 5 shows the response spectra of earthquake records used in this study.

Fig. 6 presents the hysteretic energy spectra for various target ductility ratios, in which mean values for the 20 earthquake records are plotted. The inelastic systems are assumed to have elastic–perfectly plastic force–displacement relationship. It can be observed that in structures with natural period less than about 1.0 s the hysteretic energy demand increases as the target ductility ratio increases. However the opposite is true for structures with natural period larger than 1.0 s. This phenomenon can be explained by Fig. 7 where it is depicted that in structures with short natural period the area enclosed by the hysteresis loop increases with ductility

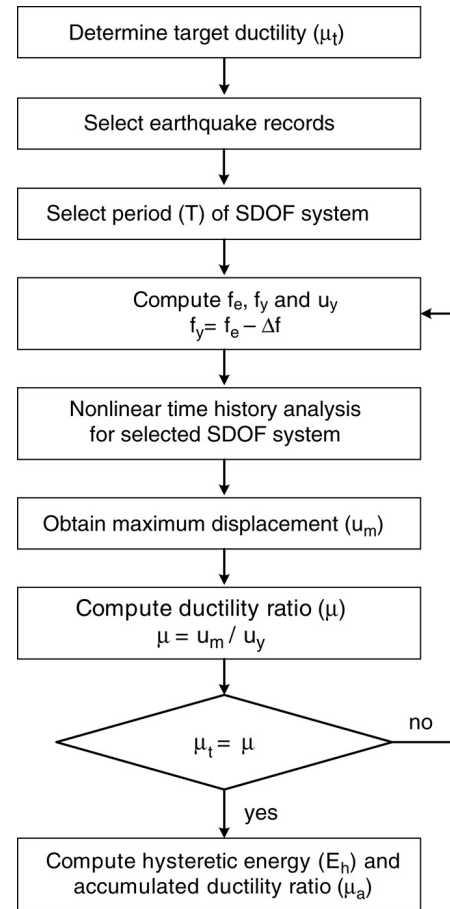


Fig. 4. Flow-chart of constructing hysteretic energy and accumulated ductility spectra.

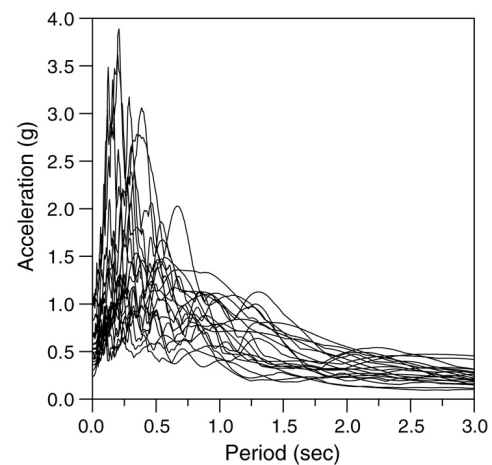


Fig. 5. Response spectra of earthquake records used in the analysis.

ratio, whereas in structures with long natural period the area decreases with increasing ductility ratio.

Fig. 8 shows the averaged accumulated ductility spectra plotted for various target ductility ratios constructed using the 20 earthquake records used previously. From the figure it can be noticed that the accumulated ductility ratios are nearly constant in structures with natural period of longer than about 0.1 s. According to the results of experiments conducted at

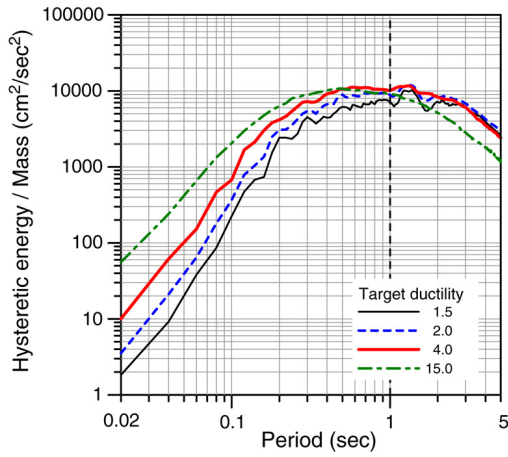
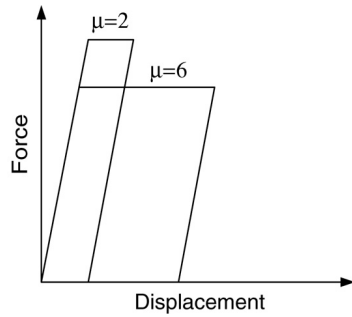
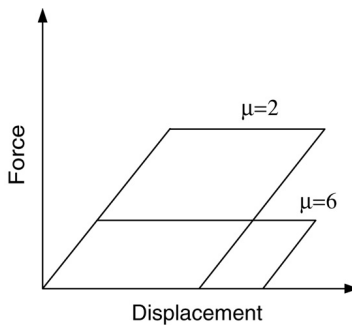


Fig. 6. Constant ductility hysteretic energy spectra.



(a) Short period structures.



(b) Long period structures.

Fig. 7. Change in area enclosed by hysteresis loop.

the University of California at Berkeley [15], the maximum ductility ratio of BRB reaches as high as 20 before failure occurs. Therefore the accumulated ductility of 20 ~ 70 observed in the figure for the target ductility ratio of 15 seems to be reasonable.

4. Design procedure

In this section the procedure for the proposed energy-based design method is summarized. The proposed procedure is derived based on the assumption that the gravity load-resisting system, the frame consisting of hinge-connected beams and columns, is already designed to remain elastic during earthquake, and all the seismic input energy is dissipated

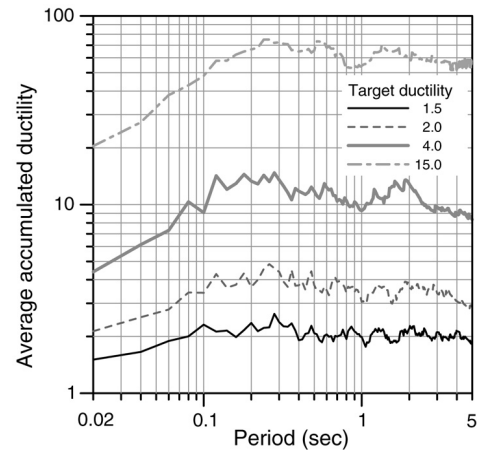


Fig. 8. Accumulated ductility spectra for various target ductility ratios.

by BRB. Therefore in this study the design procedure is limited to the design of BRB. It is also assumed that the hysteretic energy and the accumulated ductility spectra for given earthquake excitation are already prepared.

Step 1. Determination of target ductility ratio

The yield displacement of BRB can be computed from yield stress and the length of the brace as follows:

$$u_{by} = \frac{1}{\cos \theta} \frac{L_b}{E_b} \sigma_{by} \quad (1)$$

where θ , L_b , and E_b are the slope, length, and the elastic modulus of BRB, respectively. Once the target displacement u_T is determined, the target ductility ratio is obtained as:

$$\mu_t = \frac{u_T}{u_{by}}. \quad (2)$$

Step 2. Assumption of natural period

In the first stage of design the natural period of the structure needs to be assumed. In this study the following equation adopted by IBC-2000 [17] for the braced frame is used:

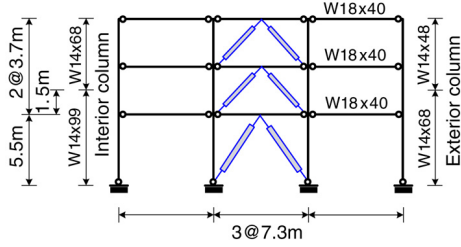
$$T = 0.0488 H^{3/4}. \quad (3)$$

Step 3. Required size of BRB

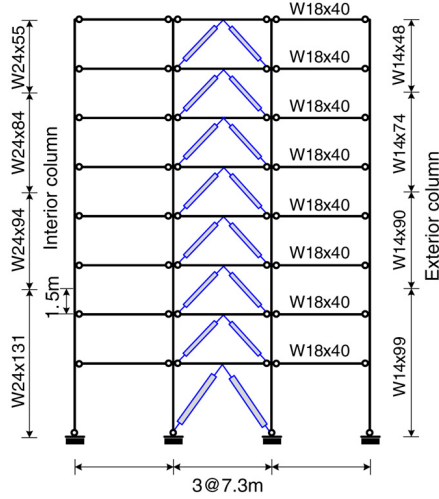
The cross-sectional area of BRB required to meet the given target displacement is obtained by equating the hysteretic energy demand to the plastic energy dissipated by BRB:

$$E_h \times \sum_{i=1}^N m_i = \sum_{j=1}^N F_{yj} u_{yj} (\mu_a - 1) = (\mu_a - 1) \times \sum_{j=1}^N A_{bj} \sigma_{by} \frac{L_{bj} \sigma_{by}}{E_b} \quad (4)$$

where E_h , F_{yj} , u_{yj} , and μ_a are the hysteretic energy obtained from the spectrum, yield force of the j th story, yield displacement of the j th story, and the accumulated ductility ratio, respectively. Also A_{bj} , L_{bj} , θ_j , σ_{by} , and E_b are the cross-sectional area, length, slope, and yield stress of BRB located on the j th story, respectively. The cross-sectional area of BRB located in the j th story, A_{bj} , is denoted by the cross-sectional



(a) Three-story structure.



(b) Eight-story structure.

Fig. 9. Model structures with BRB.

area of BRB in the first story, A_{b1} , multiplied by the story-wise distribution ratio, DR_j :

$$A_{bj} = DR_j A_{b1}. \quad (5)$$

Then from Eqs. (4) and (5) the cross-sectional area of BRB in the first story, A_{b1} , can be expressed as:

$$A_{b1} = \frac{E_h \sum_{i=1}^N m_i}{(\mu_a - 1) \sum_{j=1}^N DR_j \sigma_{by} \frac{L_{bj} \sigma_{by}}{E_b}}. \quad (6)$$

Once the size of BRB in the first story is determined, those in the other stories can be obtained using Eq. (5).

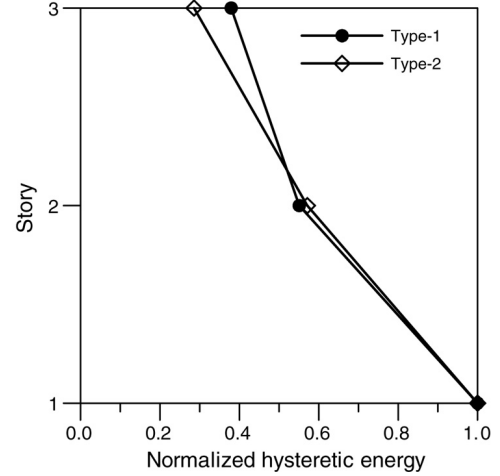
Step 4. Finalization of the BRB size

The size of BRB determined above is based on the natural period assumed by Eq. (3). As we have the first trial values of BRB size now, eigenvalue analysis can be carried out to compute the more precise natural period for the structure. The process is repeated until the natural period converges.

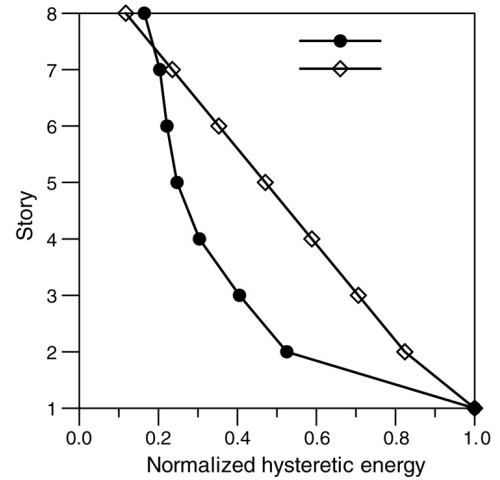
5. Application of the design procedure

5.1. Model structures

The three-bay three- and eight-story framed structures with V-shaped BRB shown in Fig. 9 are prepared for analysis. The



(a) Three-story structure.



(b) Eight-story structure.

Fig. 10. Story-wise hysteretic energy distribution ratio.

bay length of each model structure is 7.3 m, the height of the story is 5.5 m in the first story and 3.7 m in the other stories. The mass of each story is 1538 kN and the inherent modal damping ratios are assumed to be 2% of the critical damping. Beams and columns were designed strong enough so that they remain elastic for gravity load and the forces induced by the earthquake load. The member cross-sectional dimensions of the model structures are presented in the figure.

5.2. Design of buckling-restrained braces

The required size of BRB to meet the target displacement was computed by equating the hysteretic energy demand to the plastic energy dissipated by braces obtained from the accumulated ductility spectrum. The story-wise distribution ratio of the hysteretic energy, DR_j , was both computed from dynamic analysis (Type-1) and from simplified triangular distribution form (Type-2). To obtain a Type-1 distribution pattern, the model structures were analyzed using the twenty earthquake records. Fig. 10 shows that the two distribution types are similar in the three-story structure, but are quite

Table 1

Natural period, hysteretic energy, accumulated ductility ratio, and BRB cross-sectional area of the three-story structure determined in each trial

Trial	1	2	3	4
Period (s)	0.330	0.536	0.519	0.517
E_h (kN cm)	9432.9	10 399.4	10 495.2	10 495.2
μ_a	70.84	73.21	73.26	73.26
A_{b1} (cm ²)	57.90	61.74	62.27	62.27
A_{b2} (cm ²)	31.90	34.01	34.30	34.30
A_{b3} (cm ²)	21.98	23.44	23.64	23.64

Table 2

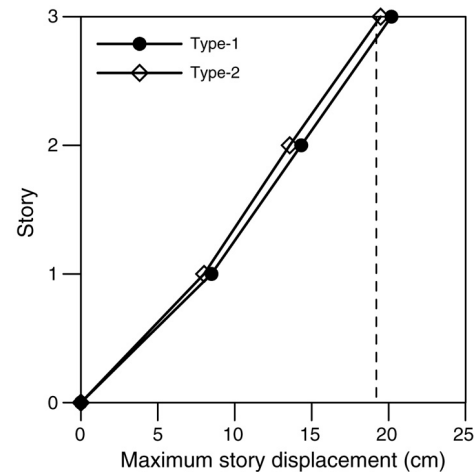
Final values of BRB cross-sectional area (cm²)

Story	3 Story		8 Story	
	Type-1	Type-2	Type-1	Type-2
8	–	–	30.46	19.64
7	–	–	37.71	39.28
6	–	–	41.07	58.92
5	–	–	45.80	78.56
4	–	–	56.29	98.21
3	47.27	36.81	75.06	117.85
2	68.60	73.61	97.25	137.49
1	124.54	128.82	185.23	166.95
Summation	240.41	239.23	568.88	716.90

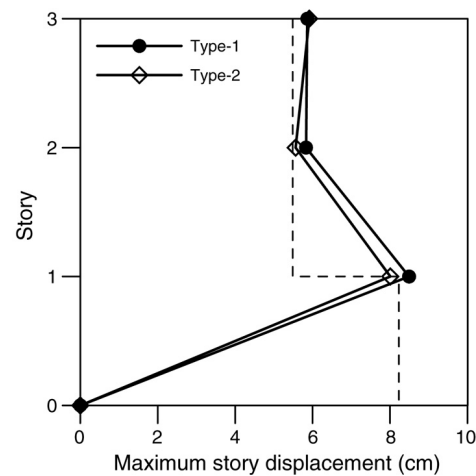
different in the eight-story structure. The target inter-story drift is taken to be 1.5% of the story height; then the target ductility ratios, determined from Eqs. (1) and (2), result in 14.9 and 15.1 for the three- and eight-story structures, respectively. Therefore a target ductility ratio of 15 is used to obtain hysteretic energy demand and accumulated ductility ratio from the spectra. The required cross-sectional area of BRB is computed using those spectra following the proposed design method. Table 1 presents the natural period, hysteretic energy, accumulated ductility ratio, and the cross-sectional area of a single BRB determined in each iteration in the three-story structure when the Type-1 pattern was used. Table 2 presents the final values for the BRB size in model structures for the two story-wise distribution types. From the table it can be observed that the results are similar regardless of the story-wise distribution pattern of BRB in the three-story structure. However in the eight-story structure the total amount of BRB turned out to be much smaller when a Type-1 distribution pattern was used.

5.3. Verification of the design

Time history analyses were carried out using the nonlinear analysis program code DRAIN-2D+ [18] to verify the validity of the proposed design method. A total of 20 earthquake records used previously to construct the hysteretic energy and accumulated ductility spectra were used again in the analyses. According to the analysis results plotted in Figs. 11 and 12, the mean values for the top story displacements of the model structures correspond well with the target displacements. Also, the inter-story drifts turned out to be relatively uniform over the structure height, which is quite



(a) Story displacements.



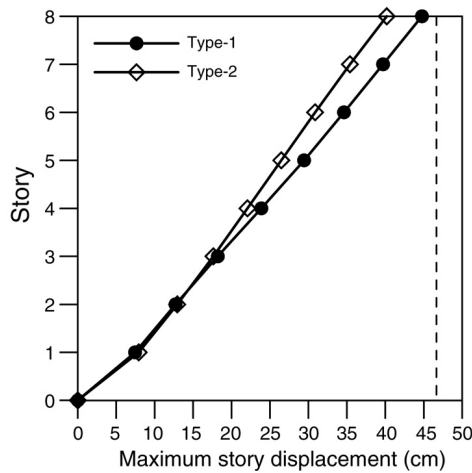
(b) Inter-story drifts.

Fig. 11. Maximum responses of the three-story structure.

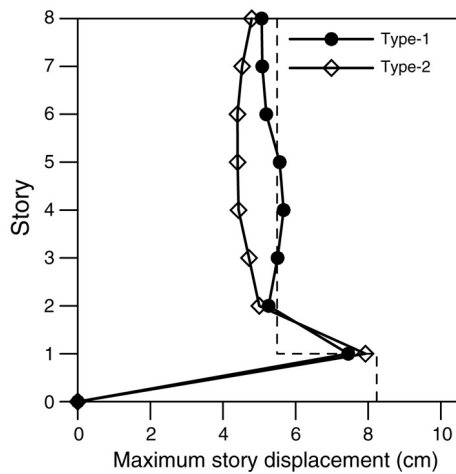
desirable because uniform inter-story drifts indicate uniform damage distribution. No discernable difference could be observed in the displacement responses between Type-1 and Type-2 story-wise energy distribution patterns. Fig. 13 plots the hysteretic energy dissipated in each story of the model structures. Mean values of the twenty results were plotted for the two different story-wise distribution patterns. It can be observed that there is no significant difference between Type-1 and Type-2 story-wise energy distribution patterns. In the eight-story structure, the Type-1 distribution results in a more uniform story-wise distribution of hysteretic energy. Generally the hysteretic energy distribution shape is closer to the Type-1 distribution pattern.

6. Conclusions

In this study the energy-based seismic design procedure for framed structures with buckling-restrained braces was proposed using hysteretic energy spectra and accumulated ductility spectra. According to the time-history analysis results the maximum displacements of the model structures with

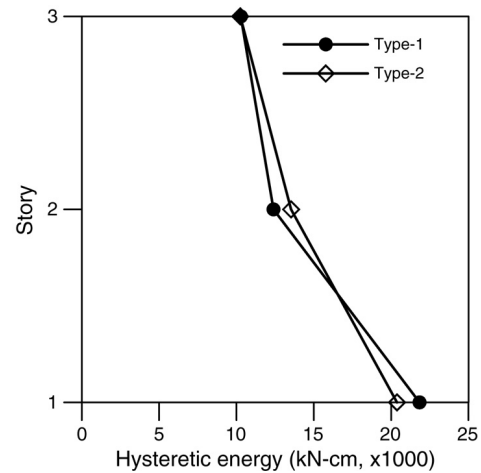


(a) Story displacements.

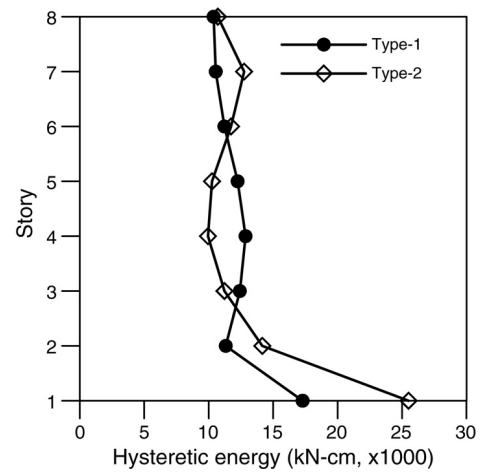


(b) Inter-story drifts.

Fig. 12. Maximum responses of the eight-story structure.



(a) Three-story structure.



(b) Eight-story structure.

Fig. 13. Story-wise distribution of hysteretic energy in the three-story structure.

BRB designed in accordance with the proposed method coincided well with the target displacements in the three-story structure. In the eight-story structure the results were somewhat on the conservative side. It was also shown that the story-wise distribution of hysteretic energy, which indicates the distribution of structural damage, was relatively uniform throughout the story.

It should be noted, however, that the proposed method of energy-based design, which utilizes the hysteretic energy and the accumulated ductility spectrum constructed from analysis of SDOF systems, may only be applied to low- to medium-rise structures, because the hysteretic energy of a high-rise structure may be quite different from that of the equivalent SDOF structure due to higher mode effects.

Acknowledgement

This work was supported by the Ministry of Construction and Transportation (grant No. C103A1040001-03A0204-00110). This financial support is gratefully acknowledged.

References

- [1] Housner G. Limit design of structures to resist earthquakes. In: Proceedings of the first world conference on earthquake engineering. 1956.
- [2] Uang CM, Bertero VV. Use of energy as a design criterion in earthquake-resistant design. Report No. UCB/EERC-88/18. Earthquake Engineering Research Center, University of California at Berkeley; 1988.
- [3] Estes KR, Anderson JC. Hysteretic energy demands in multistory buildings. In: Seventh US national conference on earthquake engineering. 2002.
- [4] Riddell R, Garcia JE. Hysteretic energy spectrum and damage control. *Earthquake Engineering and Structural Dynamics* 2001;30(12):1791–816.
- [5] Léger P, Dussault S. Seismic-energy dissipation in MDOF structures. *Journal of Structural Engineering, ASCE* 1992;118(5):1251–69.
- [6] Akbas B, Shen J, Hao H. Energy approach in performance-based seismic design of steel moment resisting frames for basic safety objective. *The Structural Design of Tall Buildings* 2001;10(3):193–217.
- [7] Leelataviwat S, Goel SC, Stojadinović B. Energy-based seismic design of structures using yield mechanism and target drift. *Journal of Structural Engineering, ASCE* 2002;128(8):1046–54.
- [8] Dasgupta P, Goel SC, Parra-Montesinos G, Tsai TC. Performance-based seismic design and behavior of a composite buckling restrained braced frame. In: 13th world conference on earthquake engineering. 2004.

- [9] Kim J, Choi H, Chung L. Energy-based seismic design of structures with buckling-restrained braces. *Steel and Composite Structures* 2004;4(6): 639–706.
- [10] Akiyama H. Earthquake-resistant limit-state design for building. Tokyo (Japan): The University of Tokyo Press; 1985.
- [11] Fajfar P, Vidic T, Fischinger M. Seismic design in medium- and long-period structures. *Earthquake Engineering and Structures Dynamics* 1989; 18(8):1133–44.
- [12] Manfredi G. Evaluation of seismic energy demand. *Earthquake Engineering and Structures Dynamics* 2001;30(4):485–99.
- [13] Fajfar P, Vidic T. Consistent inelastic design spectra: Hysteretic and input energy. *Earthquake Engineering and Structures Dynamics* 1994;23(5): 523–37.
- [14] Huang YH, Wada A, Sugihara H, Narikawa M, Takeuchi T, Iwata M. Seismic performance of moment resistant steel frame with hysteretic damper. In: *Proceedings of the third international conference STESSA*. 2000.
- [15] Black C, Makris N, Aiken I. Component testing, stability analysis and characterization of buckling restrained unbonded braces. Report No. PEER-2002/08. Pacific Earthquake Engineering Research Center, University of California at Berkeley; 2002.
- [16] Somerville P, Smith H, Puriyamurthala S, Sun J. Development of ground motion time histories for phase 2 of the FEMA/SAC steel project. SAC Joint Venture, SAC/BD-97/04; 1997.
- [17] International Code Council. 2000 International building code. In: *International conference of building officials*. 2000.
- [18] Tsai KC, Li JW. DRAIN2D+, A general purpose computer program for static and dynamic analyses of inelastic 2D structures supplemented with a graphic processor. Report No. CEER/R86-07. Taipei (Taiwan): National Taiwan University; 1997.